AJNR

Brain Network Architecture and Global Intelligence in Children with Focal Epilepsy

M.J. Paldino, F. Golriz, M.L. Chapieski, W. Zhang and Z.D. Chu

AJNR Am J Neuroradiol 2017, 38 (2) 349-356
doi: https://doi.org/10.3174/ajnr.A4975
http://www.ajnr.org/content/38/2/349

Brain Network Architecture and Global Intelligence in Children with Focal Epilepsy

M.J. Paldino, F. Golriz, M.L. Chapieski, W. Zhang, and Z.D. Chu

ABSTRACT

BACKGROUND AND PURPOSE: The biologic basis for intelligence rests to a large degree on the capacity for efficient integration of information across the cerebral network. We aimed to measure the relationship between network architecture and intelligence in the pediatric, epileptic brain.

MATERIALS AND METHODS: Patients were retrospectively identified with the following: 1) focal epilepsy; 2) brain MR imaging at 3T, including resting-state functional MR imaging; and 3) full-scale intelligence quotient measured by a pediatric neuropsychologist. The cerebral cortex was parcellated into approximately 700 gray matter network "nodes." The strength of a connection between 2 nodes was defined by the correlation between their blood oxygen level–dependent time-series. We calculated the following topologic properties: clustering coefficient, transitivity, modularity, path length, and global efficiency. A machine learning algorithm was used to measure the independent contribution of each metric to the intelligence quotient after adjusting for all other metrics.

RESULTS: Thirty patients met the criteria (4–18 years of age); 20 patients required anesthesia during MR imaging. After we accounted for age and sex, clustering coefficient and path length were independently associated with full-scale intelligence quotient. Neither motion parameters nor general anesthesia was an important variable with regard to accurate intelligence quotient prediction by the machine learning algorithm. A longer history of epilepsy was associated with shorter path lengths ($P = .008$), consistent with reorganization of the network on the basis of seizures. Considering only patients receiving anesthesia during machine learning did not alter the patterns of network architecture contributing to global intelligence.

CONCLUSIONS: These findings support the physiologic relevance of imaging-based metrics of network architecture in the pathologic, developing brain.

ABBREVIATIONS: BOLD = blood oxygen level–dependent; IQ = intelligence quotient

Epilepsy is a common neurologic condition defined by recurrent, unprovoked seizures that affect 1% of the population, including 1 in 200 children.[1] In contrast to epilepsies encountered in the adult population, developmental lesions are the most frequent source of medically intractable seizures in children.[2] Surgical resection in the setting of such focal epilepsies represents an attractive management option.[3] However, even in the most highly selected cohorts, outcomes remain highly variable.[4] Evidence suggests that such inconsistencies may reflect so-called "focal" epilepsies being, in many cases, associated with extensive alterations of the cerebral network.[3,5,6]

With advances in MR imaging, the architecture of the cerebral network is now accessible to systematic study.[7] Resting-state functional MR imaging, which measures the blood oxygen level–dependent (BOLD) signal with time, is one method by which a neural network can be constructed. Because the sequence is task-free, it is of great potential value to young or developmentally impaired children, in whom cooperation with task-based functional imaging and neuropsychological evaluation may not be possible. Regions of the brain that interact to contribute a given function continue to exhibit similar BOLD fluctuations at rest.[8] Hence, with resting-state fMRI, the strength of a connection between brain regions is inferred on the basis of the degree of correlation between their BOLD signal time courses. Connectivity defined in this manner can then be used to create a comprehensive

Received March 28, 2016; accepted after revision August 29.

From the Departments of Radiology (M.J.P., F.G., Z.D.C.) and Psychology (M.L.C.) and Outcomes and Impact Service (W.Z.), Texas Children's Hospital, Houston, Texas.

Paper previously presented at: Annual Meeting of the American Society of Neuroradiology, May 21–26, 2016; Washington, DC.

Please address correspond Michael J. Paldino, MD, Texas Children's Hospital, Department of Radiology, 6621 Fannin St, Houston, TX 77030; e-mail: Michael.paldino@gmail.com

http://dx.doi.org/10.3174/ajnr.A4975

map of connections in the brain.[7] Within this framework, the brain is represented as a collection of "nodes," or anatomic elements in the network, and the connection between each pair of nodes is represented by an "edge."

Once constructed, the architecture of the network can be summarized at the whole-brain scale according to graph theory.[9] An array of graph theory metrics has been described, each of which has the potential to capture specific topologic features of the network.[9] In general terms though, most metrics measure, in some way, the degree to which the network supports either integration across or functional subspecialization within the brain. Previous studies using network metrics derived from resting-state fMRI have demonstrated differences from normal in various disease states, including epilepsy.[10-14] More recently, incremental "dose-response" relationships between brain network efficiency, as quantified by graph theory, and global intelligence have been reported in both adults[15,16] and healthy children.[17] Although these findings point to the potential for network metrics to provide physiologically meaningful markers of cognitive function, few data exist regarding these relationships in the pathologic setting. Nor is it known whether such markers maintain their physiologic meaning when imaging is performed with the patient under general anesthesia, a state of consciousness known to alter neurovascular coupling and BOLD synchrony.[18]

The goals of this study were 2-fold: to determine which metrics of global network architecture are most closely related to intelligence in the pediatric, epileptic brain; and to determine whether such relationships continue to emerge when functional images are acquired with the patient under anesthesia.

MATERIALS AND METHODS

This Health Insurance Portability and Accountability Act–compliant study was approved by the local institutional review board. Informed consent was waived. Patients were identified retrospectively from the medical record with the following inclusion criteria: 1) pediatric age group (21 years of age or younger); 2) diagnosis of focal epilepsy[19] by a pediatric epileptologist based on clinical history and seizure semiology; 3) MR imaging of the brain performed at 3T, including a resting-state fMRI sequence; and 4) full-scale intelligence quotient (IQ) measured according to an age-appropriate version of the Wechsler Intelligence Scales administered by a pediatric neuropsychologist within 3 months of the MR imaging. Refinements to the above-defined population were planned on the basis of the following exclusions: 1) any brain operation performed before the MR imaging, and 2) motion or other artifactual degradation of image quality.

MR Imaging

All imaging was performed on a 3T Achieva system (Philips Healthcare, Best, the Netherlands) with a 32-channel phased array coil. We obtained the following sequences: 1) structural images: sagittal volumetric T1-weighted images (TR/TE, 7.2/2.9 ms; 1 acquisition; flip angle, 7°; TI, 1100 ms; FOV, 22 cm; voxel, 1 × 1 × 1 mm); 2) resting-state fMRI: axial single-shot EPI fMRI (TR/TE, 2000/30 ms; flip angle, 80°; 1 acquisition; FOV, 24 cm; matrix, 64 × 64; voxel, 3.75 × 3.75 × 3.75 mm; 300 volumes; duration, 10 minutes) performed in the resting state. Patients not receiving anesthesia during the examination were instructed to lie quietly in the scanner with their eyes closed. All images were visually inspected for artifacts, including susceptibility and subject motion.

Image Processing and Analysis

Network Node Definition. A processing pipeline was implemented by using Matlab scripts (Version 7.13; MathWorks, Natick, Massachusetts), in which adapter functions were embedded to execute FreeSurfer reconstruction (Version 5.3.0; http://surfer.nmr.mgh.harvard.edu), and several tools in the FSL suite (http://www.fmrib.ox.ac.uk/fsl).[20] First, reconstruction of cerebral cortical surfaces was performed on the T1 structural image by using FreeSurfer. This processing stream includes motion correction, skull stripping, intensity normalization, segmentation of white matter and gray matter structures, parcellation of the gray matter–white matter boundary, and surface deformation following intensity gradients, which optimally place the gray matter/white matter and gray matter/CSF borders at the location where the greatest shift in intensity defines the transition between tissue classes.[21,22] FreeSurfer outputs were visually inspected for accuracy by using the FreeView software (http://surfer.nmr.mgh.harvard.edu), to assure appropriate placement of the pial and gray-white surfaces for each patient.

Next, a self-developed Matlab program was applied to the FreeSurfer outputs, including the pial and gray-white surfaces, to further subdivide the 75 standard parcels according to their surface area (as defined on the FreeSurfer gray-white surface mesh). During this process, each cortical parcel was iteratively divided into 2 new parcels of equal size until the surface area of each parcel was less than a predefined threshold value of 350 mm^2. Each surface parcel was then converted into a volume mask of gray matter at that region; each resulting volume of interest formed a node on the network. The number of nodes in each patient's network ranged from 539 to 841 (mean, 690.7 ± 66.3).

Network Edge Definition. The first 5 images in each resting-state sequence were discarded to allow magnetization to reach equilibrium. Preprocessing and independent component analysis of the functional datasets were performed by using FSL MELODIC (http://fsl.fmrib.ox.ac.uk/fsl/fslwiki/MELODIC), including motion correction, section-timing correction, brain extraction, spatial smoothing (Gaussian kernel of full width at half maximum of 5 mm), and high-pass temporal filtering equivalent to a wavelength of 100 seconds (0.01 Hz). Noise related to motion and other physiologic nuisance was addressed according to an independent component analysis technique.[23] Nonsignal components were removed manually by an expert operator with 5 years of experience using independent component analysis in this patient population. Although the optimal strategies for noise removal in fMRI remain the subject of debate,[24,25] an independent component analysis technique was selected because it has been shown to minimize the impact of motion on network metrics while, at the same time, decreasing the loss of temporal *df* and preserving the signal of interest across a variety of resting-state datasets.[24] Motion parameters measured during preprocessing were summarized for each patient as "translation" (the root mean

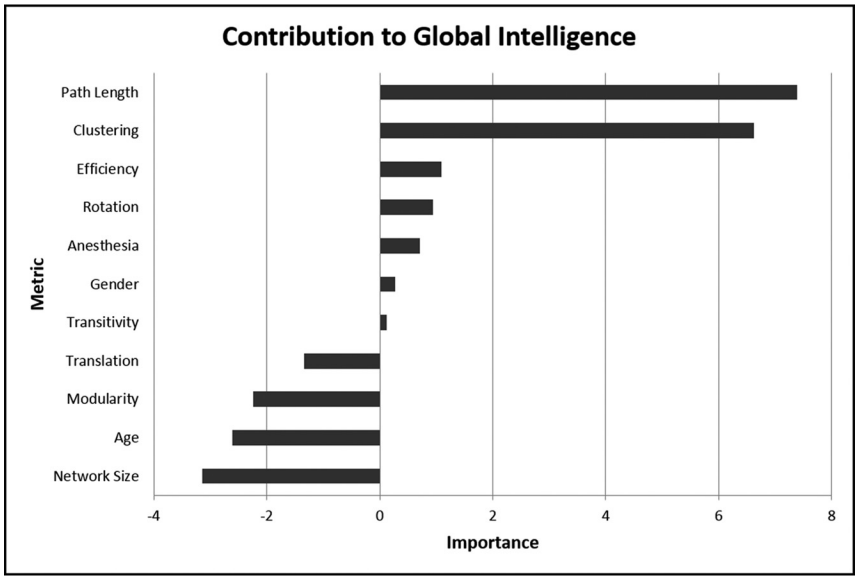

FIG 1. The importance of global metrics of network architecture with respect to full-scale intelligence quotient. The independent contribution of each metric was estimated as the error of the prediction of IQ of the machine learning algorithm compared with the error that results when that metric is negated. The most negative value of importance defines the limit of noise. Hence, variables with importance greater in magnitude than the most negative variable are significant.

Table 1: Metrics of network architecture

Metric	Description
Clustering coefficient	The fraction of the nodes of a given neighbor that are also neighbors of each other; reflects segregation/subspecialization in the network
Transitivity	The fraction of node triplets in the network that form a completely connected triangle; reflects segregation/functional subspecialization in the network
Modularity	The degree to which nodes tend to segregate into relatively independent modules; reflects segregation/subspecialization within the network
Characteristic path length	Minimum number of edges required to traverse the distance between 2 nodes averaged over the network; reflects the ease of information transfer across the network
Global efficiency	Inverse of the mean characteristic path length averaged over the network; reflects integration in the network

square of the 3 translational parameters) and "rotation" (root mean square of 3 rotational parameters). These translation and rotation estimates were then included as covariates in the machine learning analysis (see below). The functional image volume for each patient was registered to that individual's skull-stripped structural T1 dataset by using the FMRIB Linear Image Registration Tool (FLIRT; http://www.fmrib.ox.ac.uk). The inverse transformation matrix was calculated in this step and was subsequently used to transform all masks from structural to functional space. All registrations were inspected for accuracy. Voxelwise BOLD signal time-series were averaged over each node. The strength of an edge (connection) between 2 nodes was specifically defined as the absolute value of the Pearson correlation coefficient between their BOLD time-series.

Graph Construction and Network Metric Calculation. Weighted, undirected connection matrices were constructed, consisting of the pair-wise correlation between BOLD time-series over all network nodes (see an example in Fig 1). Graphs for each patient were thresholded according to a Bonferroni-corrected P value as follows[26]: 1) The P value for each pair-wise correlation in the connection matrix was multiplied by $(N^2 - N) / 2$ to correct for multiple comparisons, and 2) edges with a corrected P value $> .05$ were then set to zero.

For each weighted, undirected connection matrix, the following topologic properties were calculated by using Matlab scripts provided in The Brain Connectivity Toolbox (http://www.brain-connectivity-toolbox.net): clustering coefficient, transitivity, modularity, characteristic path length, and global efficiency. A brief description for each metric is provided in Table 1. To account for the differences in brain volume, and therefore intrinsic network size, that are inherent to a pediatric population, we normalized each raw network metric to the corresponding metric computed on a random network of identical size.[27]

Statistical Analyses

Statistical testing was performed by using the R statistical software package, Version 3.0.2 (http://www.r-project.org). A machine learning method was used to quantify the independent contribution of the measured network metrics to global intelligence. In other words, the importance of each network metric was computed after adjusting for the contribution of all other network metrics (as well as for age, sex, translational and rotational motion [measured during fMRI preprocessing in FSL], and the use of anesthesia during MR imaging). This analysis was accomplished by using a random forest approach, which has been previously described in detail.[28] In short, this ensemble learning method operates by constructing a multitude of decision trees during training and outputting the mean of predictions from individual trees. It is based on bootstrap aggregating, or bagging, in which numerous models are fitted during individual bootstrap samples and then are combined by averaging. During training, approximately one-third of the cohort is omitted at random from the training set: This omitted portion of the dataset is considered "out-of-bag." The IQ of each individual held out of bag is then predicted on the basis of the "learned" model. This process is repeated 1000 times, each time with a new, randomly selected out-of-bag cohort. The independent contribution of an individual variable is estimated by measuring the error for IQ prediction in the out of bag cohort compared with the error that results when that particular variable is negated during bagging. This method was

selected for 1 main reason: Other statistical methods, including regression, generate a model based on data from a given cohort and then assess the fit of the model on the same individuals. This machine learning algorithm, by contrast, tests the predictive capacity of the generated model on a subset of the cohort held out of bag. In other words, the capacity of the model to predict IQ is tested in a previously unseen subset of patients. Machine learning approaches, therefore, represent an attractive method by which metrics derived from quantitative imaging can be assessed with respect to their potential translation into clinically meaningful information at the level of a single patient.[29]

For all variables deemed important above, the relationships to global intelligence were further quantified by using linear regression. The goal of this step was not to confirm the importance of the variables above but rather to demonstrate graphically the nature of the relationships measured by the machine learning algorithm. A potential relationship between important variables and the span of epilepsy history was also assessed by linear regression.

Finally, the impact of anesthesia on the relationship between network architecture and intelligence was interrogated as follows: 1) the Wilcoxon rank sum test (corrected for multiple comparisons) was used to assess potential differences in network metrics between sedated and nonsedated patients (corrected $\alpha = .05$); 2) the machine learning analysis was repeated, this time only considering the subset of patients who underwent anesthesia during the MR imaging examination; and 3) for variables deemed important in step 2, the relationships to global intelligence were again demonstrated graphically by using linear regression.

Table 2: Anesthetic medications administered during MR imaging

Drug Combination	No. of Patients	Age Range (median) (yr)
Propofol only	9	9–17 (11)
Propofol + sevoflurane	6	8–16 (14)
Propofol + Dex	4	4–19 (15)
Propofol + sevoflurane + Dex	1	11–11 (11)
None	10	9–19 (16)

Note:—Dex indicates dexmedetomidine.

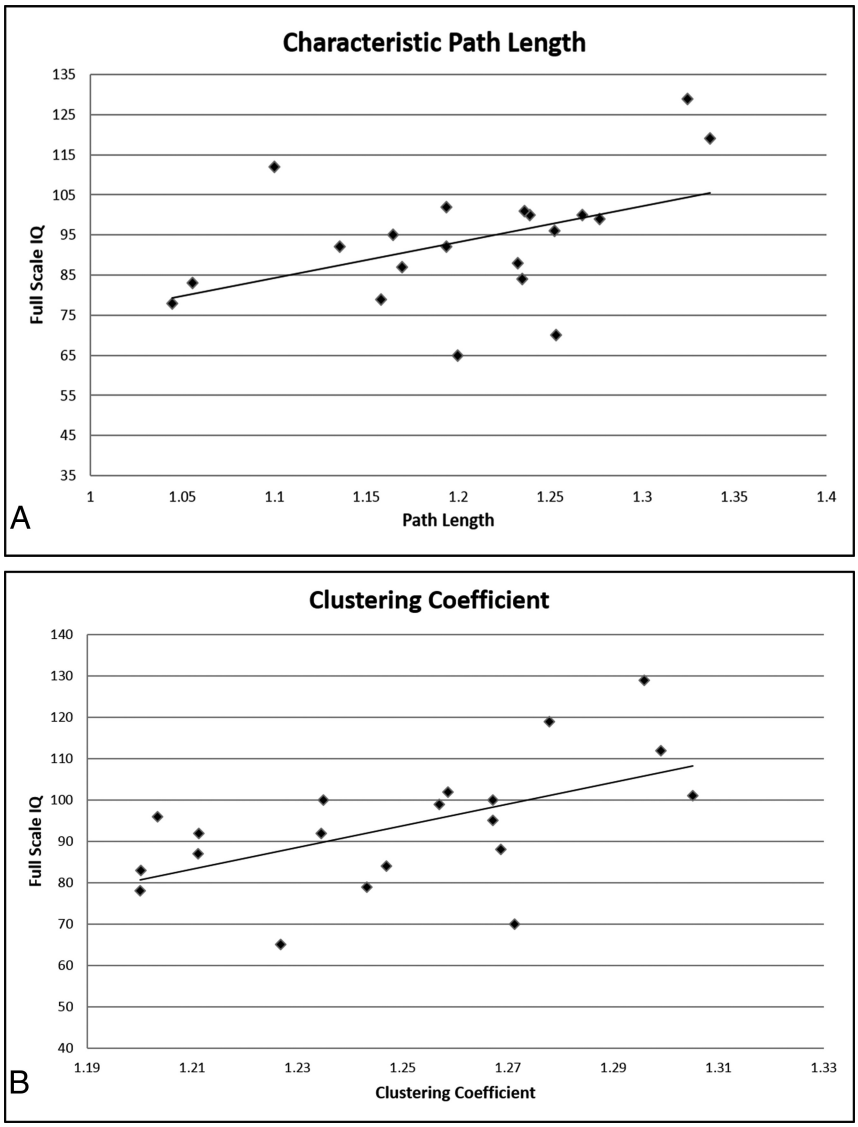

FIG 2. Graphic representation of the relationships of path length (*A*) and clustering coefficient (*B*) to the full-scale intelligence quotient.

RESULTS

Patients

Imaging was performed from June 2013 to June 2015. Forty patients met the inclusion criteria. Ten were excluded on the basis of prior brain surgery. Thirty patients with focal epilepsy (age range, 4–18 years; median age, 13 years; 15 males) composed the final study group. Of this cohort, 5 patients had structurally normal brains and 25 patients had demonstrable structural abnormalities at MR imaging, including focal cortical dysplasia ($n = 9$), mesial temporal sclerosis ($n = 6$), low-grade tumor ($n = 4$), a single epileptogenic tuber in the setting of tuberous sclerosis ($n = 3$), subependymal gray matter heterotopia ($n = 1$), hypothalamic hamartoma ($n = 1$), and prior hypoxic-ischemic insult ($n = 1$). An age-appropriate version of the Wechsler Intelligence Scales was successfully administered in all patients; full-scale intelligence quotient in the cohort ranged from 49 to 129 (median, 88). Of the total study group, 20 patients required general anesthesia during the imaging examination on the basis of guidelines from the American Academy of Pediatrics.[30] The specific medications administered during MR imaging are provided in Table 2.

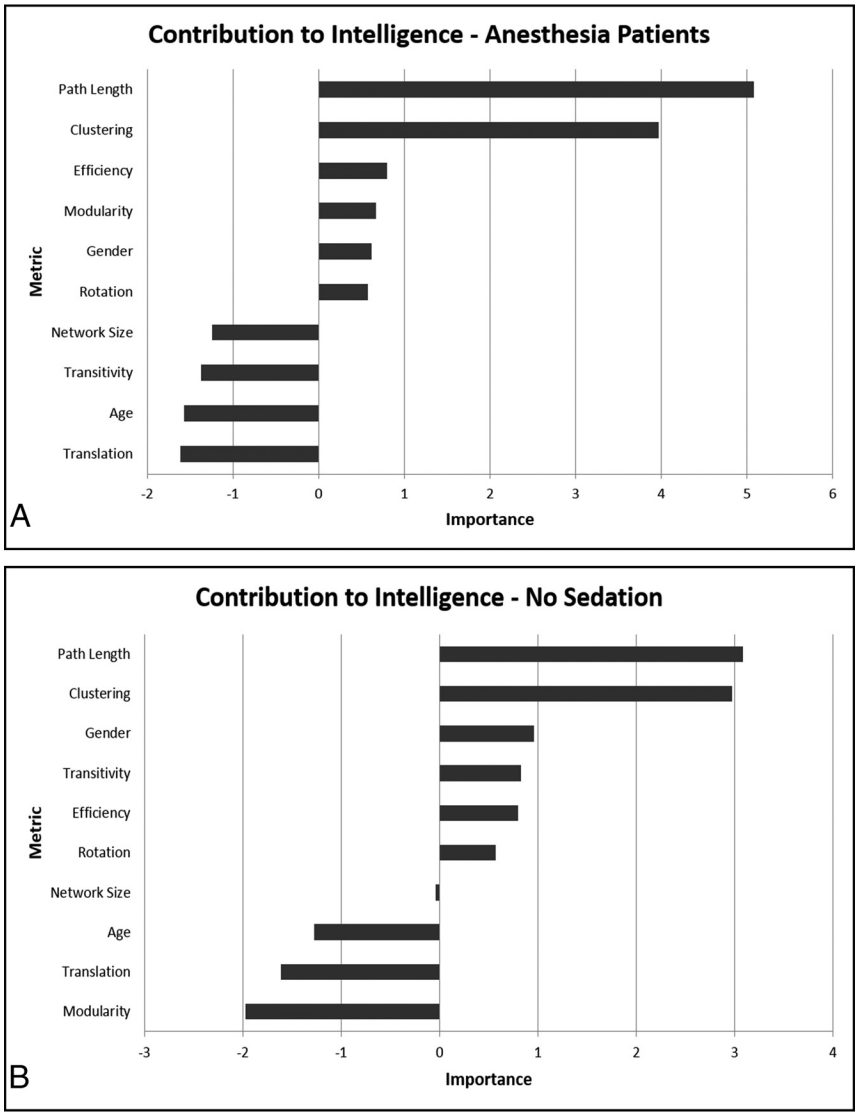

FIG 3. The importance of global metrics of network architecture with respect to the full-scale intelligence quotient for patients requiring anesthesia (*A*) and those who were nonsedated (*B*).

Network Architecture and Intelligence

All brains demonstrated small-world organization, characterized by high clustering coefficients and path lengths approaching those of a random graph. In general terms, both segregation (functional subspecialization) and integration in the network were important contributors to global brain function. In particular, after accounting for age and sex, the clustering coefficient and path length were independently associated with full-scale IQ (Fig 1). Both clustering coefficient ($r = 271$; $P = .0018$) and path length ($r = 107$; $P = .0016$) were directly related to full-scale IQ (Fig 2). Notably, neither motion parameters nor general anesthesia was an important variable with regard to accurate IQ prediction by the machine learning algorithm (Fig 1). Network size (the number of nodes in a patient's network) similarly did not impact the relationship between metrics and IQ (Fig 1). A longer history of epilepsy was associated with shorter path lengths ($P = .008$), consistent with reorganization of the network on the basis of seizures. Clustering coefficient, by contrast, was not related to seizure history ($P = .81$).

Regarding the potential impact of general anesthesia on the utility of network construction, network metrics in patients who required anesthesia during MR imaging did not differ significantly from those in nonsedated patients (P range, .51–.87). Furthermore, considering only patients requiring anesthesia during machine learning did not alter the patterns of network architecture contributing to global intelligence (Fig 3). Finally, for the entire cohort, clustering coefficient ($r = 262$; $P = .01$) and path length ($r = 89$; $P = .04$) were both directly related to full-scale IQ in this subset of children (Fig 4).

DISCUSSION

We report 2 main findings in children with focal epilepsy: 1) Two metrics of network architecture, clustering coefficient and path length, were independently associated with full-scale IQ; and 2) these relationships between network architecture and global intelligence persisted in patients whose functional images were acquired while they were under general anesthesia.

Most higher order functions of the human brain are not accomplished by individual functional centers compartmentalized to a particular region of the cortex. Rather, they emerge from parallel processing within subspecialized but distributed functional systems. A complex neural network, formed by some 10^{10} neurons, forms the structural substrate for efficient interaction between local and distributed areas of the cerebrum. Within this network, segregation into relatively independent local neighborhoods provides an architectural framework for functional subspecialization. Yet a complete range of function only emerges from efficient integration of these subspecialized neighborhoods across the entire brain. While these 2 properties might seem to be mutually antagonistic—efficient integration is best supported by a random network with a high proportion of long-range edges (short path length), while segregation requires a network with primarily local connections (high clustering coefficient)—the recent description of small-world networks by Watts and Strogatz[31] has provided critical insight toward resolving this inconsistency. They observed that within the framework of mathematic models, the addition of a small number of long-range connections to a locally connected graph has little effect on the clustering coefficient but reduces the path length to approximately that of a random graph. In graph theoretic terms, then, small-world networks have both high clustering coefficients, like regular networks, and short path lengths, like random networks. Hence,

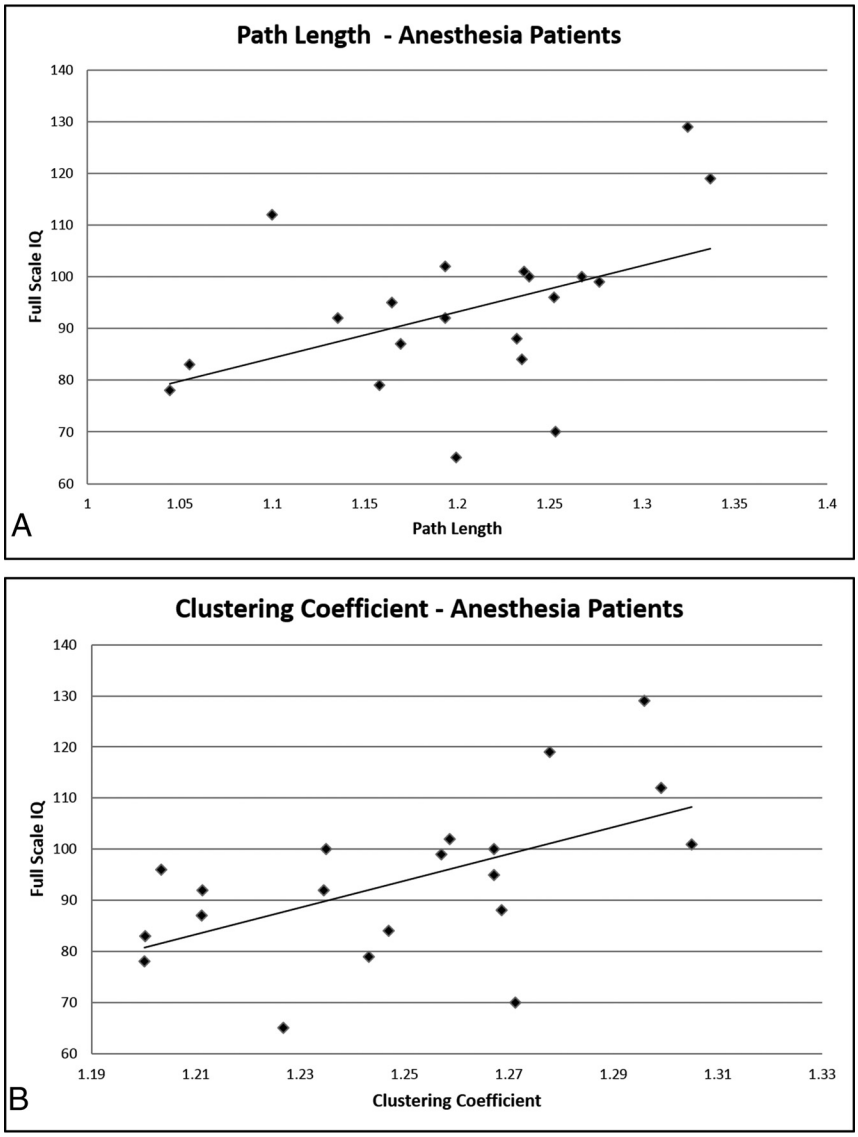

FIG 4. Graphic representation of the relationships of path length (*A*) and clustering coefficient (*B*) to full-scale intelligence quotient for patients requiring anesthesia.

small-world organization is an effective means by which both functional subspecialization and integration can be concomitantly supported by the same network. It has been suggested that small-world properties and the resulting efficiency of the network constitute the biologic underpinnings of cognitive function in the human brain.[15,17,32] We observed that both segregation (clustering coefficient) and integration (path length) were important features of the network with regard to global intelligence, consistent with this idea. In addition, these same relationships were detected in the subset of patients anesthetized according to various drug regimens that included propofol. This last point has important implications for both the pediatric and epilepsy populations, many of whom require anesthesia during MR imaging acquisition. Together, our findings suggest that the metrics of network architecture have the capacity to probe physiologically relevant features of the neural network in a clinical population of children with epilepsy.

In our cohort, shorter path lengths were associated with lower full-scale IQ scores. This relationship was largely mediated by seizure history; a long history of epilepsy portended short path length, suggesting that ongoing seizures are associated with rewiring of the cerebral network. These findings reinforce the idea that network metrics in epileptic brains may not have the same physiologic meaning as in healthy subjects. Synaptic efficacy, according to the Hebbian theory on neural plasticity, arises from repeat and persistent stimulation.[33] In this manner, connections contributing to useful and efficient subnetworks are strengthened with time, while those associated with less functional/inefficient networks are pruned.[34] In the setting of epilepsy, however, synapses are strengthened along pathways related to seizure propagation, essentially hijacking Hebbian processes.[35] Connectivity in this setting is potentiated without regard to network function, resulting in aberrant and potentially maladaptive pathways.[36,37] Consistent with this idea, Liao et al[38] observed shorter path lengths, also related to seizure history, in young adults with temporal lobe epilepsy. Our findings suggest that similar network reorganization occurs in the pediatric population and, furthermore, that such alterations are indeed maladaptive. In an older cohort of adult patients, Vlooswijk et al[39] observed increased path lengths in patients with cryptogenic localization–related epilepsy. Together these findings raise the possibility that the impact of seizures on the cerebral network may be exaggerated in young patients, whose cellular processes are primed to allow cerebral growth and reorganization.

To our knowledge, these are the first data using network architecture as a marker for full-scale IQ in children with epilepsy. However, our results are consistent with work in healthy adults[15,16] and children[17] that has demonstrated consistent relationships between network architecture and intelligence. As discussed above, the specific nature of these relationships is likely to reflect the pathophysiologic mechanisms at play in a given patient population. Hence, at any given time point, an individual's network will reflect not only the trajectories of normal brain development but also the cumulative impact of their particular CNS pathology. Previous studies have reported global network abnormalities in both adults[38-40] and children[41,42] with localization-related epilepsies. Our results extend this previous work to provide evidence that such network reorganization is physiologically meaningful with respect to brain function.

The question of general anesthesia is a complicated one

because it can be accomplished according to a variety of drug regimens, each of which may have a different effect on resting-state networks.[43] Of particular relevance to our work, several groups have reported a relative decrease in connectivity within frontoparietal[44] and whole-brain[45] networks during propofol-induced loss of consciousness. However, these studies did not include an assessment of how well the topology of the constructed brain networks paralleled their ultimate function. Our work suggests that despite relative changes that likely occur with regard to the intrinsic characteristics of the resting-state signal, the resulting network construction retains the capacity to capture important physiologic features of the cerebral network. This idea is consistent with the findings of Liu et al,[46] whose work with electrocorticography has suggested that long-range coordination of neural activity within large-scale brain networks is a core aspect of the physiology of the brain and does not depend on the state of consciousness.

This study has several limitations. First, it was conducted in a cohort of pediatric patients with focal epilepsy. Generalization of these results to patients with other CNS disorders, or to adults with epilepsy, may not be valid. Second, due to the study design, it was not possible to evaluate the relative changes in resting-state raw signal and the resulting functional networks that occurred after loss of consciousness under anesthesia. Along similar lines, due to the small number of patients in each group, the impact of different drug regimens (and their respective doses) on network construction could not be interrogated. Thus, although the physiologic relevance of network metrics was retained across the population, the possibility remains that the use of anesthesia altered, at least in relative fashion, the observed relationships. We also cannot exclude the possibility that anesthesia may completely abrogate accurate network reconstruction in some subsets of individual patients. However, the purpose of this study was not to define the exact impact of anesthetic agents on resting-state networks. Rather, we sought to determine whether it is generally feasible to obtain physiologically relevant information from images acquired with the patient under anesthesia according to the general clinical workflow within a radiology department. Future inquiry regarding the specific drug regimens that allow construction of networks that most closely parallel the true physiology of the brain would be of great future value to this field of study.

CONCLUSIONS

We report 2 main findings in children with focal epilepsy: 1) Metrics of network architecture derived from resting-state functional networks were important contributors to full-scale IQ, and 2) the relationships between network architecture and intelligence were robust to general anesthesia. Our results suggest that imaging-based markers of network architecture indeed capture physiologically relevant information with regard to the function of the pathologic brain and, furthermore, that this information can be acquired with the patient under general anesthesia. In sum, our findings support the potential for resting-state fMRI to provide clinically meaningful markers of network function in children with epilepsy.

REFERENCES

1. Boyle CA, Decouflé P, Yeargin-Allsopp M. **Prevalence and health impact of developmental disabilities in US children.** *Pediatrics* 1994; 93:399–403 Medline
2. Phi JH, Cho BK, Wang KC, et al. **Longitudinal analyses of the surgical outcomes of pediatric epilepsy patients with focal cortical dysplasia.** *J Neurosurg Pediatr* 2010;6:49–56 CrossRef Medline
3. Duchowny M. **Clinical, functional, and neurophysiologic assessment of dysplastic cortical networks: implications for cortical functioning and surgical management.** *Epilepsia* 2009;50(suppl 9):19–27 CrossRef Medline
4. Westerveld M, Sass KJ, Chelune GJ, et al. **Temporal lobectomy in children: cognitive outcome.** *J Neurosurg* 2000;92:24–30 CrossRef Medline
5. Duchowny M, Jayakar P, Levin B. **Aberrant neural circuits in malformations of cortical development and focal epilepsy.** *Neurology* 2000;55:423–28 Medline
6. Yasuda CL, Valise C, Saude AV, et al. **Dynamic changes in white and gray matter volume are associated with outcome of surgical treatment in temporal lobe epilepsy.** *Neuroimage* 2010;49:71–79 CrossRef Medline
7. Hagmann P, Cammoun L, Gigandet X, et al. **Mapping the structural core of human cerebral cortex.** *PLoS Biol* 2008;6:e159 CrossRef Medline
8. Biswal BB, van Kylen J, Hyde JS. **Simultaneous assessment of flow and BOLD signals in resting-state functional connectivity maps.** *NMR Biomed* 1997;10:165–70 Medline
9. Rubinov M, Sporns O. **Complex network measures of brain connectivity: uses and interpretations.** *Neuroimage* 2010;52: 1059–69 CrossRef Medline
10. He H, Sui J, Yu Q, et al. **Altered small-world brain networks in schizophrenia patients during working memory performance.** *PLoS One* 2012;7:e38195 CrossRef Medline
11. Göttlich M, TF, Heldmann M, et al. **Altered resting state brain networks in Parkinson's disease.** *PLoS One* 2013;8:e77336 CrossRef Medline
12. Brier MR, Thomas JB, Fagan AM, et al. **Functional connectivity and graph theory in preclinical Alzheimer's disease.** *Neurobiol Aging* 2014;35:757–68 CrossRef Medline
13. Sanz-Arigita EJ, Schoonheim MM, Damoiseaux JS, et al. **Loss of 'small-world' networks in Alzheimer's disease: graph analysis of FMRI resting-state functional connectivity.** *PLoS One* 2010;5: e13788 CrossRef Medline
14. van Diessen E, Zweiphenning WJ, Jansen FE, et al. **Brain network organization in focal epilepsy: a systematic review and meta-analysis.** *PLoS One* 2014;9:e114606 CrossRef Medline
15. Li Y, Liu Y, Li J, et al. **Brain anatomical network and intelligence.** *PLoS Comput Biol* 2009;5:e1000395 CrossRef Medline
16. van den Heuvel MP, Stam CJ, Kahn RS, et al. **Efficiency of functional brain networks and intellectual performance.** *J Neurosci* 2009;29: 7619–24 CrossRef Medline
17. Kim DJ, Davis EP, Sandman CA, et al. **Children's intellectual ability is associated with structural network integrity.** *Neuroimage* 2016; 124(pt A):550–56 CrossRef Medline
18. Peltier SJ, Kerssens C, Hamann SB, et al. **Functional connectivity changes with concentration of sevoflurane anesthesia.** *Neuroreport* 2005;16:285–88 CrossRef Medline
19. Berg AT, Berkovic SF, Brodie MJ, et al. **Revised terminology and concepts for organization of seizures and epilepsies: report of the ILAE Commission on Classification and Terminology, 2005–2009.** *Epilepsia* 2010;51:676–85 CrossRef Medline
20. Smith SM, Jenkinson M, Woolrich MW, et al. **Advances in functional and structural MR image analysis and implementation as FSL.** *Neuroimage* 2004;23(suppl 1):S208–19 CrossRef Medline
21. Fischl BL, Liu A, Dale AM. **Automated manifold surgery: constructing geometrically accurate and topologically correct models of the human cerebral cortex.** *IEEE Trans Med Imaging* 2001;20:70–80 CrossRef Medline

22. Fischl B, Salat DH, van der Kouwe AJ, et al. **Sequence-independent segmentation of magnetic resonance images.** *Neuroimage* 2004: (suppl 1):S69–84 CrossRef Medline
23. Thomas CG, Harshman RA, Menon RS. **Noise reduction in BOLD-based fMRI using component analysis.** *Neuroimage* 2002;17: 1521–37 CrossRef Medline
24. Pruim RH, Mennes M, Buitelaar JK, et al. **Evaluation of ICA-AROMA and alternative strategies for motion artifact removal in resting state fMRI.** *Neuroimage* 2015;112:278–87 CrossRef Medline
25. Bright MG, Murphy K. **Is fMRI "noise" really noise? Resting state nuisance regressors remove variance with network structure.** *Neuroimage* 2015;114:158–69 CrossRef Medline
26. Weisstein E. Bonferroni Correction**.** From MathWorld–A Wolfram Web Resource. http://mathworld.wolfram.com/BonferroniCorrection.html. Accessed August 5, 2016
27. Rubinov M, Sporns O. **Weight-conserving characterization of complex functional brain networks.** *Neuroimage* 2011;56: 2068–79 CrossRef Medline
28. Breiman L. **Random forests.** *Machine Learning* 2001;45:5–32 CrossRef
29. Paldino MJ, Hedges K, Zhang W. **Independent contribution of individual white matter pathways to language function in pediatric epilepsy patients.** *Neuroimage Clin* 2014;6:327–32 CrossRef Medline
30. Coté CJ, Wilson S; American Academy of Pediatrics; American Academy of Pediatric Dentistry. **Guidelines for monitoring and management of pediatric patients before, during, and after sedation for diagnostic and therapeutic procedures: update 2016.** *Pediatrics* 2016;138:pii: e20161212 CrossRef Medline
31. Watts DJ, Strogatz SH. **Collective dynamics of 'small-world' networks.** *Nature* 1998;393:440–42 CrossRef Medline
32. Pamplona GS, Santos Neto GS, Rosset SR, et al. **Analyzing the association between functional connectivity of the brain and intellectual performance.** *Front Hum Neurosci* 2015;9:61 CrossRef Medline
33. Chaudhury S, Sharma V, Kumar V, et al. **Activity-dependent synaptic plasticity modulates the critical phase of brain development.** *Brain Dev* 2016;38:355–63 CrossRef Medline
34. Cruikshank SJ, Weinberger NM. **Evidence for the Hebbian hypothesis in experience-dependent physiological plasticity of neocortex: a critical review.** *Brain Res Brain Res Rev* 1996;22:191–228 CrossRef Medline
35. Hernan AE, Holmes GL, Isaev D, et al. **Altered short-term plasticity in the prefrontal cortex after early life seizures.** *Neurobiol Dis* 2013; 50:120–26 CrossRef Medline
36. Galicia E, Imai K, Mohamed IS, et al. **Changing ictal-onset EEG patterns in children with cortical dysplasia.** *Brain Dev* 2009;31:569–76 CrossRef Medline
37. Koh S, Mathern GW, Glasser G, et al. **Status epilepticus and frequent seizures: incidence and clinical characteristics in pediatric epilepsy surgery patients.** *Epilepsia* 2005;46:1950–54 CrossRef Medline
38. Liao W, Zhang Z, Pan Z, et al. **Altered functional connectivity and small-world in mesial temporal lobe epilepsy.** *PLoS One* 2010;5: e8525 CrossRef Medline
39. Vlooswijk MC, Vaessen MJ, Jansen JF, et al. **Loss of network efficiency associated with cognitive decline in chronic epilepsy.** *Neurology* 2011;77:938–44 CrossRef Medline
40. DeSalvo MN, Douw L, Tanaka N, et al. **Altered structural connectome in temporal lobe epilepsy.** *Radiology* 2014;270:842–48 CrossRef Medline
41. Vaessen MJ, Braakman HM, Heerink JS, et al. **Abnormal modular organization of functional networks in cognitively impaired children with frontal lobe epilepsy.** *Cereb Cortex* 2013;23:1997–2006 CrossRef Medline
42. Widjaja E, Zamyadi M, Raybaud C, et al. **Disrupted global and regional structural networks and subnetworks in children with localization-related epilepsy.** *AJNR Am J Neuroradiol* 2015;36:1362–68 CrossRef Medline
43. Kalthoff D, Po C, Wiedermann D, et al. **Reliability and spatial specificity of rat brain sensorimotor functional connectivity networks are superior under sedation compared with general anesthesia.** *NMR Biomed* 2013;26:638–50 CrossRef Medline
44. Boveroux P, Vanhaudenhuyse A, Bruno MA, et al. **Breakdown of within- and between-network resting state functional magnetic resonance imaging connectivity during propofol-induced loss of consciousness.** *Anesthesiology* 2010;113:1038–53 CrossRef Medline
45. Monti MM, Lutkenhoff ES, Rubinov M, et al. **Dynamic change of global and local information processing in propofol-induced loss and recovery of consciousness.** *PLoS Comput Biol* 2013;9:e1003271 CrossRef Medline
46. Liu X, Yanagawa T, Leopold DA, et al. **Robust long-range coordination of spontaneous neural activity in waking, sleep and anesthesia.** *Cereb Cortex* 2015;25:2929–38 CrossRef Medline